

SMALL SCALE MODEL ANALYSIS OF
REINFORCED CONCRETE BEAMS IN FLEXURE
AND IN TORSION

by

GARY E. MASON

B. S. in C. E., Kansas State University, 1964

A MASTER'S THESIS

submitted in partial fulfillment of the

requirements for the degree

MASTER OF SCIENCE

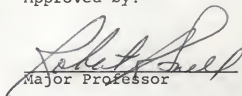
Department of Civil Engineering

KANSAS STATE UNIVERSITY

Manhattan, Kansas

1967

Approved by:


Major Professor

2668
74
1967
M399
6.2

TABLE OF CONTENTS

SUMMARY 1

INTRODUCTION. 2

REVIEW OF LITERATURE. 3

MATERIALS AND PROCEDURES USED TO DETERMINE MATERIALS
AND SPECIMEN PROPERTIES 6

 Procedures for Fabricating Specimens for
 Determining Material Properties. 6

 Procedures for Strength Testing of Model
 Test Specimens 7

 Presentation of Data Obtained From Strength
 Testing of Model Test Specimens. 8

 Properties of Wire Used to Simulate
 Reinforcing Bars 8

FLEXURE TESTING PROGRAM 18

 Review of Ultimate Strength Theory 18

 Design of Experiment for Flexure Tests 20

 Results from Quality Control Tests 21

 Procedures Used in the Flexure Tests 24

 Analysis of Results from Flexure Experiment. 28

 Conclusions Based on Flexure Experiment. 37

TORSION TESTING PROGRAM 38

 Review of Lessig's Theory. 38

 Design of Experiment for Torsion Tests 47

 Results from Quality Control Tests 48

 Procedures Used in the Torsion Tests 49

 Analysis of Results from Torsion Experiment. 56

 Conclusions Based on Torsion Experiment. 64

GENERAL CONCLUSIONS	69
RECOMMENDATIONS FOR FURTHER RESEARCH.	70
LIST OF SYMBOLS	72
ACKNOWLEDGEMENTS.	73
BIBLIOGRAPHY.	74
APPENDIX A.	77

FIGURES AND TABLES

Fig. 1 -	Loading configuration for flexure specimens	7
Fig. 2 -	Stress-strain curve for Ultracal 30 Mix	9
Table 1	Results from compression and modulus of rupture specimens	10
Table 2	Analysis of compression specimens used to design the mix.	11
Fig. 3 -	Stress-strain curve for #6 rod used in flexure beams	13
Fig. 4 -	Stress-strain curve for #6 rod used in torsion beams	14
Fig. 5 -	Stress-strain curve for black annealed wire used in torsion beams.	16
Fig. 6 -	Stress-strain curve for bright basic wire used in torsion beams.	17
Fig. 7 -	Internal forces at failure of cross-section in flexure.	19
Table 3	Design of experiment for flexure test	21
Table 4	Compressive strength of control samples for flexure tests	22
Table 5	Modulus of rupture of control samples for flexure tests	23
Table 6	Analysis of variance for quality control samples for flexure beams	25
Fig. 8 -	Typical cross-sections of flexure specimens	26
Fig. 9 -	Loading configuration of flexure specimens. . . .	27
Fig. 10-	Flexure specimen in testing machine	27
Table 7	Analysis of load cell readings of flexure beams	29
Table 8	Ultimate failure moments of flexure beams	32

Fig. 11-	Flexure specimens after failure	33
Fig. 12-	Plot of load cell readings versus span for flexure specimens	35
Table 9	Comparison of observed and calculated results for flexure beams	36
Fig. 13-	Free body of beam under combined bending and torsion	39
Fig. 14-	Compression zone at failure of beam under combined bending and torsion.	40
Table 10	Design of experiment for torsion test	48
Table 11	Compressive strength of control samples for torsion tests	50
Table 12	Modulus of rupture of control samples for torsion tests	51
Table 13	Analysis of variance for quality control samples for torsion beams	52
Fig. 15-	Typical cross-sections of torsion beams	53
Fig. 16-	Torsion specimen in testing apparatus	54
Table 14	Analysis of load cell readings of torsion beams	58
Table 15	Measured and calculated moments for torsion beams	60
Fig. 17-	Crack patterns of torsion specimens	61
Fig. 18-	Plot of load cell readings versus m for torsion specimens	63
Table 16	Comparison of measured and calculated moments for torsion beams	65
Table 17	Comparison of measured and theoretical moments for torsion specimens	66
Fig. 19-	Torque-twist curves for beams 1-0.4, 1-0.5, 24 1-0.6, 1.4-0.4, 1.4-0.5, 1.4-0.6	78

SUMMARY

The primary purpose of this investigation was to determine if model reinforced concrete beams could be used experimentally to predict the behavior of prototype beams in flexure and torsion. The results of the model tests were compared with Whitney's theory for the ultimate strength of reinforced concrete beams in flexure and with Lessig's theory for the ultimate strength of reinforced concrete beams in torsion. The flexure specimens contained only longitudinal reinforcement while the torsion specimens contained longitudinal and transverse reinforcement.

The flexural experiments were designed to allow a statistical analysis of the data for certain cross-section-span combinations. The torsion experiment was designed for a range of cross-section-m combinations where m is the ratio of transverse force to longitudinal force in the reinforcing steel.

The results from the flexure tests agreed very well with Whitney's theory. The results from the torsion tests did not agree with the ultimate strength predicted by Lessig's theory.

INTRODUCTION

The use of models in research and as an aid to design has become increasingly important in recent years. As will be shown later, it has been demonstrated that the behavior of structures can be investigated both in the elastic and inelastic ranges through the use of model analysis. It was the purpose of this study to determine whether or not results from the tests, performed by the writer, on small-scale models of reinforced concrete beams could be used to predict, with sufficient accuracy, the behavior of full-scale reinforced concrete beams as determined from theoretical analysis based on well established relationships between applied load and beam behavior.

REVIEW OF LITERATURE

Whitney's (1) method for calculating the ultimate strength of reinforced concrete beams in flexure has seen wide use since its development. It serves as a firm basis for comparing the ultimate strength of model beams tested in flexure. In 1961 Onesti (2) used Whitney's method for computing the ultimate strength of plaster models.

Until 1959 a reliable theory for predicting the ultimate strength of reinforced concrete beams in torsion was not available. Lessig (3,4,5) developed equations based on measured parameters of the tested specimens to calculate the strength of a beam in pure torsion and in combined bending and torsion. Lessig used prototype beams to develop this theory. Fan (6) and Cardenas (7) used direct model analysis to investigate Lessig's theory with fairly successful results.

Burton (8) in 1964 developed a technique to study small scale models of prestressed concrete structures in the inelastic range. To achieve this objective, his experiments were directed toward the design, construction, and testing of small scale models of pretensioned, prestressed concrete beams. In order to test models of such a nature in the inelastic range, it was desirable that as close a model-prototype relationship as possible be maintained. To meet this requirement, it was necessary that the materials used in the model faithfully reproduced the behavior of the materials in the prototype structure. It was therefore necessary to find a substitute material

for use in the model which would simulate the concrete of the prototype structure. It was concluded that a mix consisting of plaster and Ottawa sand exhibited the required compressive strength.

In a study in 1964, Chao (9) investigated the application of small scale model analysis to prestressed concrete. The first part of this paper was a theoretical study of similitude requirements for determining ultimate flexure strength by models using Whitney's method, followed by a presentation of experimental results. The second part concerned the use of model beams as a device for investigation of the relationship between the ultimate flexural strength of prestressed beams and the degree of prestressing using both under-reinforced and over-reinforced prestressed beams. The results from this investigation were insufficient to draw definite conclusions.

In 1964, Fan (6) presented the results of a study on model reinforced concrete members in simple flexure and torsion. Included in this investigation were numerous control tests in connection with plaster mix design and the properties of the reinforcing steel. In addition, this series of studies also dealt with rectangular reinforced plaster model beams in pure bending and pure torsion. The experimental results of the bending tests compared quite well with the predicted behavior according to Hognestad's theory (10).

Cardenas (7) in 1965 studied the behavior of rectangular reinforced plaster model beams subjected to combined bending

and torsion. The test specimens which contained both longitudinal and web reinforcement were analyzed by Lessig's (3,4,5) theory. The test results for plain and longitudinally reinforced specimens tested in torsion were compared with the elastic and plastic theories. The experimental results agreed reasonably well with theoretical results calculated using Lessig's theory. The experimental results did not agree with either the plastic or the elastic theories.

Thus, in its brief history, model analysis of reinforced concrete members has become a useful tool for the structural engineer.

MATERIALS AND PROCEDURES USED TO DETERMINE MATERIAL AND SPECIMEN PROPERTIES

The physical properties of the model materials used were determined in order to provide a basis for a theoretical analysis with which to compare the experimental investigation. These properties are used in Whitney's theory (1) for ultimate flexural strength and in Lessig's (3,4,5) theory for ultimate torsional strength of concrete beams.

The mix used as a model substitute for concrete in this investigation consisted of 40 percent Ultracal 30, 20 percent Standard Ottawa Sand (20-30), and 40 percent local crushed limestone between the No. 8 and No. 16 sieves. The weight of water added was 33.3 percent of the weight of the Ultracal 30. The Ottawa sand was used in the air-dried condition.

The aggregate used was 3/8 in. Zeadale limestone. Two different shipments of aggregate were required. One was used to determine the properties of the mix and was used in the flexure tests while the second was used for the torsion tests. The absorption of the first shipment was 3.9 percent while for the second shipment it was 4.1 percent.

Procedures for Fabricating Specimens for Determining Material Properties

The mixing procedure consisted of oven-drying the aggregate for 48 hours followed by cooling to room temperature. The aggregate was then immersed in water for 24 hours before the specimens were cast. Immediately before the mixing, the excess

water was taken off leaving the rock plus the absorbed water plus one-half the mix water. The ingredients were placed in a mechanical mixer and mixed for 30 seconds then the remaining water was added and mixed for two minutes. The specimens were fabricated in steel forms and covered with saturated cloths. At the end of one hour the specimens were removed from the forms and covered with saturated cloths for 23 hours. After the 24 hour curing period the specimens were tested.

Procedures for Strength Testing of Model Test Specimens

Compression and modulus of rupture samples were cast. Six specimens were cast horizontally with available steel forms having dimensions of 1 x 1 x 4-in. Three specimens were tested in compression and three in flexure from each batch. Three batches were tested to determine the uniformity of properties from batch to batch. The modulus of rupture was obtained using a third-point loading as shown in in Figure 1.

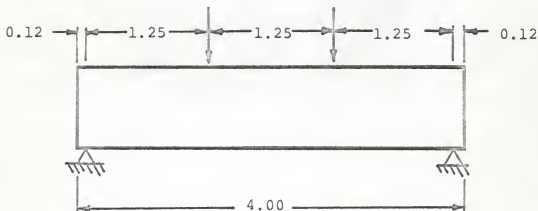


FIGURE 1. LOADING CONFIGURATION FOR SPECIMENS TESTED IN FLEXURE

Presentation of Data Obtained From Strength Testing of Model Test Specimens

A representative stress-strain curve was obtained from the nine specimens tested in compression. The strains were averaged for each stress level and the resulting stress-strain curve is shown in Figure 2 with a stress-strain curve for 3,000 psi concrete (6). Although the compressive strength of the plaster mix simulated that of 3,000 psi concrete, the stress-strain curves are not similar. The data are shown in Table 1 and the results of an analysis of variance are shown in Table 2 for the compression specimens and the modulus of rupture specimens. The results of the F-ratio test, for both compression and modulus of rupture tests, indicate that the batch-to-batch variation is not significantly greater than the within-batch variation. Thus, the specimens from all batches, for either test, can be treated as though they all came from the same batch.

Properties of Wire Used to Simulate Reinforcing Bars

The longitudinal reinforcement consisted of #6-32 threaded rod. The first number in the rod designation was the nominal diameter of the rod and the second number was the number of threads per inch. The tensile area was computed as 0.0075 square inches. As mentioned by Fan (6), the threaded rod as obtained from the producer did not exhibit a definite yield point. Therefore, it was necessary to anneal the rod before using it. Approximately 35 rods were placed on a steel frame with nuts on each end of each rod to hold the rods in place.

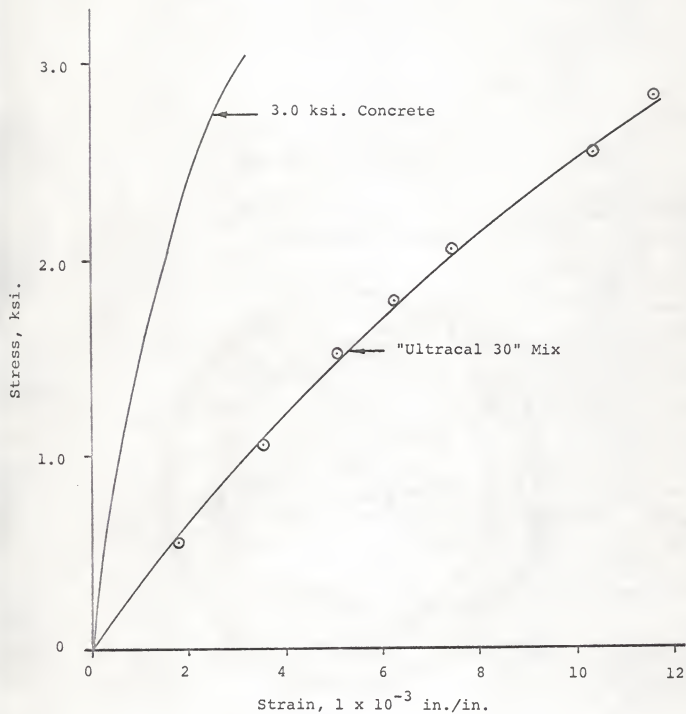


FIGURE 2. COMPRESSIVE STRESS-STRAIN CURVE FOR 3,000 PSI. CONCRETE AND FOR "ULTRACAL 30" MIX

TABLE 1

RESULTS FROM COMPRESSION AND MODULUS OF RUPTURE TESTS

		Batch Number		
Test Specimen		1	2	3
Compressive Strength, psi.	1	2855	3000	2710
	2	2690	2800	2830
	3	2790	2845	2900
Modulus of Rupture, psi.	1	414	427	402
	2	439	377	389
	3	389	452	439

TABLE 2

ANALYSIS OF SPECIMENS USED TO DESIGN THE MIX

(a) Analysis of Compression Specimens

Source	Degrees of Freedom	Sum of Squares	Mean Squares	F Test	Table F $\alpha = .05$	Significance
Between	2	19,538	9,769	0.97	5.14	No
Within	6	60,201	10,033			
Total	8	79,739				

Coefficient of Variation = 3.54 percent Grand Average = 2,821 psi.

(b) Analysis of Modulus of Rupture Specimens

Source	Degrees of Freedom	Sum of Squares	Mean Squares	F Test	Table F $\alpha = .05$	Significance
Between	2	112.9	56.45	.06	5.14	No
Within	6	5,512.7	918.78			
Total	8	5,625.6				

Coefficient of Variation = 6.40 percent Grand Average = 414 psi.

The reinforcement was placed under slight tension and placed in an oven at 950 degrees F for two hours.

Two shipments of the longitudinal reinforcement were required. Three specimens from each shipment were sampled after they were annealed. A 10-in. gage length was tested by measuring the elongation of the rod at certain loads using a dial gage. Using the method of least squares, a straight line was fitted through the linear portion of the stress-strain curve for each sample. The modulus of elasticity and the yield point were determined for each sample tested. The three values for the modulus of elasticity and yield point respectively were averaged. The idealized stress-strain curves were constructed from these average properties. The actual stress-strain curve for the first sample tested for the reinforcement for flexure beams is shown in Figure 3 along with the idealized curve for for this shipment. The actual stress-strain curve for the first of three samples tested and the idealized stress-strain curve for the reinforcing steel used in the torsion beams are shown in Figure 4.

The transverse reinforcement for the torsion beams was obtained from a local wire warehouse. For the 1 x 2-in. beams, No. 15 gage smooth black annealed wire was used. Number 15 gage bright basic wire was used for the transverse reinforcement in the 1.41 x 2.83-in. beams. The transverse reinforcement was used as obtained. The stress-strain curves for these wires were obtained using the same procedure as for the longi-

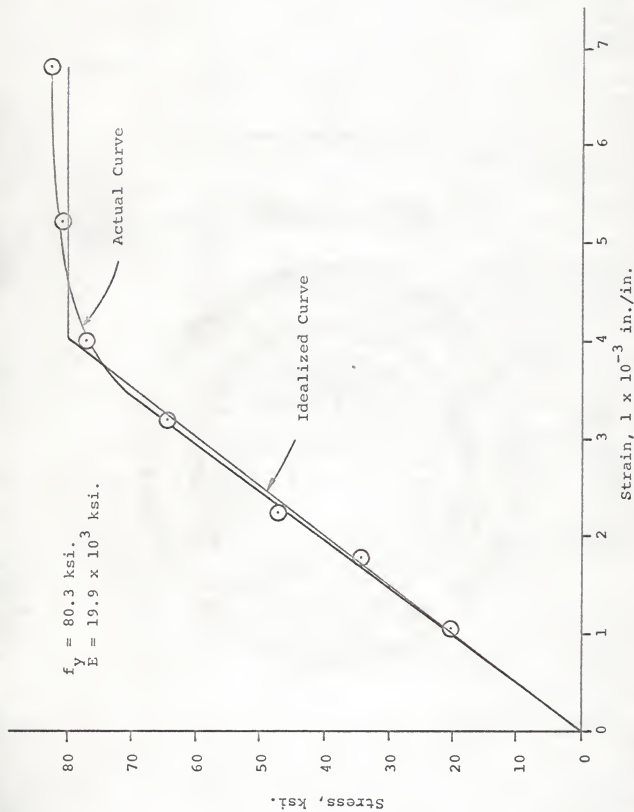


FIGURE 3. ACTUAL AND IDEALIZED STRESS-STRAIN CURVES FOR #6 THREADED ROD USED IN FLEXURE BEAMS

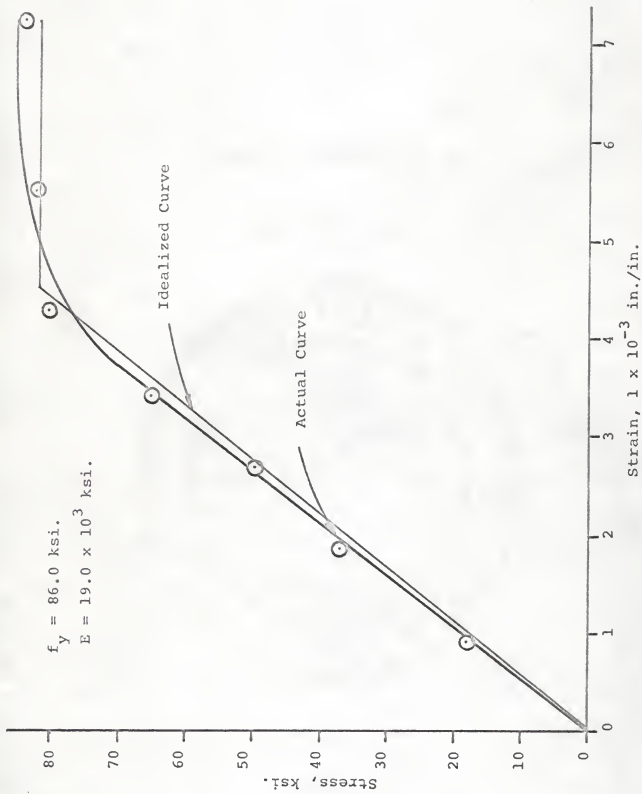


FIGURE 4. ACTUAL AND IDEALIZED STRESS-STRAIN CURVES FOR #6 THREADED ROD USED IN TORSION BEAMS

tudinal reinforcement. The stress-strain curve for a sample of the black annealed wire is shown in Figure 5 along with the idealized curve. The stress-strain curve for a sample of bright basic wire is shown in Figure 6 along with the idealized curve.

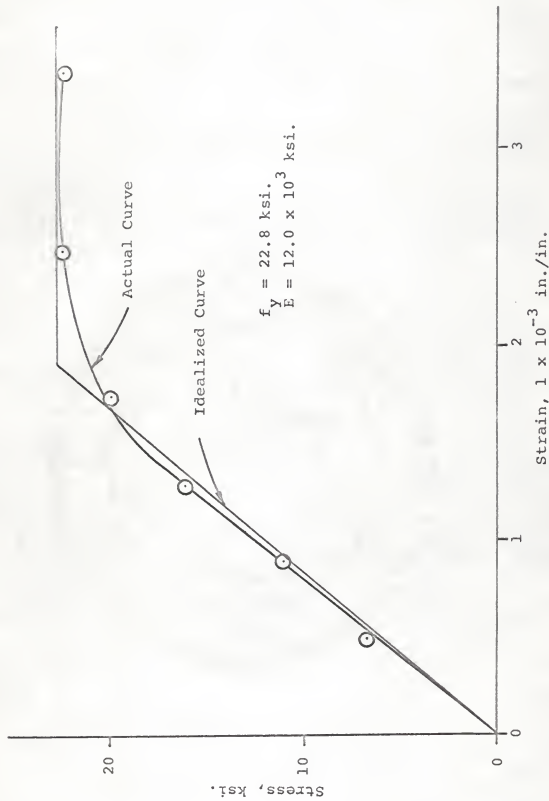


FIGURE 5. ACTUAL AND IDEALIZED STRESS-STRAIN CURVE FOR #15 GAGE BLACK ANNEALED WIRE USED AS TRANSVERSE REINFORCEMENT IN 1 x 2-IN. TORSION BEAMS



FIGURE 6. ACTUAL AND IDEALIZED STRESS-STRAIN CURVES FOR #15 GAGE BRIGHT BASIC WIRE USED AS TRANSVERSE REINFORCEMENT IN 1.41 x 2.83-IN. TORSION BEAMS

FLEXURE TESTING PROGRAM

Review of Ultimate Strength Theory

In 1937 Whitney developed a method for ultimate strength design and analysis of reinforced concrete members. This method has seen wide use since its acceptance in 1955 by the American Concrete Institute because of its simplicity and accuracy. The assumptions made by Whitney (1) are as follows:

(1) The stress-strain relationship and the distribution of compressive stress in the section is non-linear. This compressive stress distribution is replaced by one that is a simple rectangle.

(2) The uniform compressive stress in the assumed rectangular stress block is $0.85 f'_c$.

(3) The total force and the location of the neutral axis of the rectangular stress block is assumed to be the same as the actual stress block.

The internal forces in the member at failure are shown in Figure 7. The depth of the assumed compressive stress block is denoted as "a" with "b" being the width of the member.

For the cross-section to be in equilibrium the compression in the concrete must equal the tension in the reinforcing steel. Therefore,

$$0.35 f'_c ab = A_s f_y \quad (1)$$

with $p = A_s/bd$ and $e = f_y/0.85 f'_c$. Solving equation (1) for the depth of the compression zone, a, gives

$$a = epd$$

and the lever arm for the internal resisting moment as

$$\left(d - \frac{a}{2}\right) = d\left(1 - \frac{epd}{2}\right). \quad (2)$$

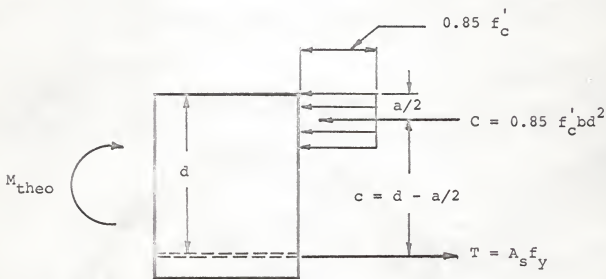


FIGURE 7. DISTRIBUTION OF INTERNAL FORCES AND STRESSES AT FAILURE

When failure is caused by yielding of the tension reinforcement, the ultimate moment is

$$M_{\text{theo}} = A_s f_y \left(d - \frac{a}{2}\right). \quad (3)$$

Equation (3) allows the ultimate flexural strength of a beam to be calculated if the beam dimensions and the strength of the steel and concrete are known.

According to Hognestad (10), failure at ultimate load by crushing the concrete occurs when the tensile steel ratio exceeds

$$p_b = \frac{0.43 f'_c}{f_y} \quad \text{to} \quad p_b = \frac{0.50 f'_c}{f_y}$$

for concrete not exceeding $f'_c = 5,000$ psi. Using Whitney's assumption, a balanced steel percentage of

$$p_b = 0.456 \frac{f'_c}{f_y} \quad (4)$$

gives

$$M_{\text{theo}} = \frac{f'_c b d^2}{3} \quad (5)$$

for the maximum moment in a beam with balanced reinforcement.

For an over-reinforced beam, Whitney suggests limiting p to the value of

$$p_{\text{max}} = \frac{0.40 f'_c}{f_y} \quad (6)$$

to prevent the use of beams whose failure in compression would be sudden and possibly catastrophic. Substituting p_{max} for p of equation (3) yields

$$M_{\text{theo}} = 0.306 f'_c b d^2 \quad (7)$$

for the ultimate moment of an over-reinforced concrete member.

Design of Experiment for Flexure Tests

The experimental program consisted of testing 18 model beams. The beams were of two sizes, namely 0.71 x 1.41-in. and 1 x 2-in. Three span lengths were tested for each of the cross-sections. These were: 18 in., 27 in., and 36 in. Three specimens were fabricated for each cross-section-span combination. The percentage of reinforcement was constant and such that the beams were under-reinforced in order to induce yielding of the steel as the mode of failure. The experimental design is shown in Table 3.

TABLE 3
DESIGN OF EXPERIMENT FOR FLEXURE TESTS

Cross Section	Span Length, in.		
	18	27	36
0.71 x 1.41-in.	1	1	1
	2	2	2
	3	3	3
1 x 2-in.	1	1	1
	2	2	2
	3	3	3

Results from Quality Control Tests

For each beam tested, four quality control samples were cast. Two were tested in compression and two in flexure. The results of the tests for quality control are shown in Table 4, for compressive strength, and in Table 5, for modulus of rupture. Confidence limits were computed for batch means using the relationship $\bar{\bar{x}} \pm ts_{\bar{x}}$ using the value for t with 17 degrees of freedom and $\alpha/2 = 0.025$.

The upper and lower compressive strength values for individual batch means, shown at the bottom of Table 4, are 2,710 psi. and 2,900 psi. The average compressive strength values for the 18 batches range from 2,710 psi. to 2,870 psi. which are within the range of values for upper and lower compressive

TABLE 4
 COMPRESSIVE STRENGTH OF QUALITY CONTROL SAMPLES FOR FLEXURE BEAMS

		Compressive Strength, psi.								
Batch	1	2	3	4	5	6	7	8	9	
Beam	1-7-18	2-7-18	3-7-18	1-7-27	2-7-27	3-7-27	1-7-36	1-7-36	3-7-36	
(1)	2,780	2,920	2,750	2,870	2,880	2,680	2,720	2,840	2,870	
(2)	2,830	2,800	2,910	2,830	2,810	2,820	2,840	2,900	2,700	
Average	2,805	2,860	2,830	2,850	2,845	2,750	2,780	2,870	2,785	
Batch	10	11	12	13	14	15	16	17	18	
Beam	1-1-18	2-1-18	3-1-18	1-1-27	2-1-27	3-1-27	1-1-36	2-1-36	3-1-36	
(1)	2,740	2,830	2,920	2,720	2,680	2,770	2,910	2,830	2,870	
(2)	2,680	2,750	2,790	2,810	2,860	2,800	2,800	2,710	2,760	
Average	2,710	2,790	2,855	2,765	2,770	2,785	2,855	2,770	2,815	

Lower Confidence Limit for batch means = 2,710 psi. ; N = 18, $\alpha/2 = 0.025$

Upper Confidence Limit for batch means = 2,900 psi. ; N = 18, $\alpha/2 = 0.025$

TABLE 5

MODULUS OF RUPTURE OF QUALITY CONTROL SAMPLES FOR FLEXURE BEAMS

		Modulus of Rupture, psi.								
Batch	1	2	3	4	5	6	7	8	9	
Beam	1-.7-18	2-.7-18	3-.7-18	1-.7-27	2-.7-27	3-.7-27	1-.7-36	2-.7-36	3-.7-36	
(1)	402	389	427	389	414	402	402	439	402	
(2)	439	427	402	427	389	427	439	389	452	
Average	422	408	415	408	402	415	421	414	427	
Batch	10	11	12	13	14	15	16	17	18	
Beam	1-1-18	2-1-18	3-1-18	1-1-27	2-1-27	3-1-27	1-1-36	2-1-36	3-1-36	
(1)	427	389	377	414	427	452	414	402	377	
(2)	377	427	402	377	402	402	427	452	414	
Average	402	408	390	396	415	427	420	427	396	

Lower Confidence Limit for batch means = 387 psi. ; N = 18, $\alpha/2 = 0.025$.

Upper Confidence Limit for batch means = 435 psi. ; N = 18, $\alpha/2 = 0.025$.

strength required for the assumption that the values obtained are no different than those that would have been obtained if all the specimens had come from a single batch for an alpha level of 0.05.

A comparison of upper and lower values of modulus of rupture, for individual batches with average values for the 18 batches, shown in Table 5, leads to the same assumption as that for compressive strength. That is, all 18 batches can be assumed to yield modulus of rupture results which are no different than the results that would have been obtained if all test specimens had come from the same batch. These assumptions are further born out in the Analysis of Variance computations shown in Table 6, where batch-to-batch differences cannot be differentiated from within-batch differences when tested at an alpha level of 0.05.

The compressive strength of the quality control samples was close to that of 3,000 psi. concrete but the modulus of rupture was slightly higher. Greater variation in the flexural strength than in the compressive strength of the control samples was expected.

Procedures Used in the Flexure Tests

Figure 8 shows the two cross-sections tested. The third-point loading configuration is shown in Figure 9. Figure 10 shows a beam in the testing machine with external stirrups in place. The external stirrups were used on the outer thirds of each specimen to prevent the beam from failing in shear. They

TABLE 6

ANALYSIS OF VARIANCE TABLES FOR QUALITY CONTROL SAMPLES FOR FLEXURE BEAMS

(a) Analysis of Variance of Compression Specimens

Source	Degrees of Freedom	Sum of Squares	Mean Squares	F Test	Table F $\alpha = .05$	Significance
Between	17	69,050	4,062	0.65	2.23	No
Within	18	111,820	6,212			
Total	35	180,870				

Coefficient of Variation = 2.56 percent

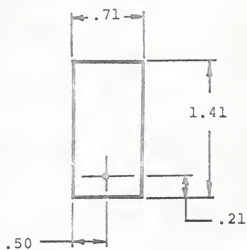
Grand Average = 2,805 psi.

(b) Analysis of Variance of Modulus of Rupture Specimens

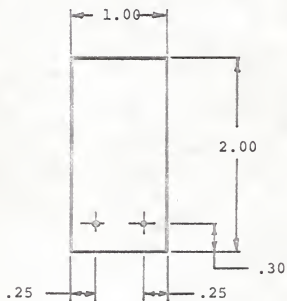
Source	Degrees of Freedom	Sum of Squares	Mean Squares	F Test	Table F $\alpha = .05$	Significance
Between	17	4,293	253	0.34	2.23	No
Within	18	13,029	724			
Total	35	17,322				

Coefficient of Variation = 5.41 percent

Grand Average = 411 psi.



(a) Typical cross-section for 0.71 x 1.41-in. beam



(b) Typical cross-section of 1 x 2-in. beam

FIGURE 8. TYPICAL CROSS-SECTION OF FLEXURE SPECIMENS

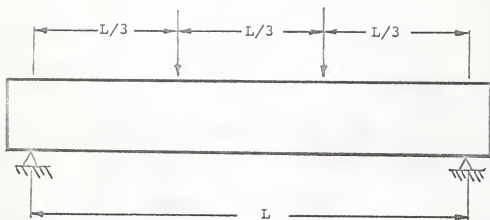


FIGURE 9. LOADING CONFIGURATION OF FLEXURE SPECIMEN



FIGURE 10. FLEXURE SPECIMEN IN TESTING MACHINE

were made from two 3/8 in. wide steel plates fastened together by 3/16 in. stove bolts to form a box stirrup which was then bolted on the specimen as shown. Loading pads 1/4 in. wide were placed under the loading points to prevent local crushing of the concrete. The applied force required for the beams to fail was measured by a load cell.

Analysis of Results from Flexure Experiment

The ultimate load cell readings are shown in Table 7 for the reinforced beams tested in flexure. An analysis of variance was performed on the load cell readings and is also shown in Table 7. The analysis of variance indicated that cross-section area, A , contributed significantly to differences observed in load cell readings. Span length, L , did not. The interaction term, $A \times L$, again contributed to observed differences.

The analysis indicates that a significant part of the variation in the load cell readings can be explained on the basis of the cross-sectional area, A . This, of course, was anticipated on the basis of well known theory concerning the behavior of reinforced concrete beams subjected to flexure. That is, according to Whitney, the theoretical failure moment of an under-reinforced concrete beam is:

$$M_{\text{theo}} = p b d f_y \left(d - \frac{a}{2} \right)$$

or

$$M_{\text{theo}} = p A f_y \left(d - \frac{a}{2} \right)$$

where p is the percentage reinforcement and A is the cross-section area of the beam.

TABLE 7

ANALYSIS OF ULTIMATE LOAD CELL READINGS OF FLEXURE BEAMS

Cross Section	Span Length, in.		
	18	27	36
	Ultimate Load Cell Readings		
.71 x 1.41-in.	225	165*	110
	230	175	105
	<u>205</u>	<u>140</u>	<u>100</u>
Average	220	160	105
Standard Deviation	13.23	18.03	5.00
Coefficient of Variation	6.02	11.28	4.76
1 x 2-in.	625	400	310
	600	410	280*
	<u>635</u>	<u>410</u>	<u>305</u>
Average	620	407	298
Standard Deviation	17.92	5.76	16.09
Coefficient of Variation	2.85	1.42	5.39

(continued on next page)

TABLE 7
ANALYSIS OF ULTIMATE LOAD CELL READINGS OF FLEXURE BEAMS
(continued)

Source	df	SS	MS	F	F $\alpha = .05$	Sign.
Cross Section, A	1	352,800	352,800	$\frac{352,800}{17,267}$	18.50	Yes
Span Length, L	2	146,033	73,016	$\frac{73,016}{17,267}$	19.00	No
A x L	2	34,534	17,267	91	3.89	Yes
Spec. in L x A cells	12	2,283	190			
Total	17	535,650				

*Remade since the plane of failure was located outside the middle third.

The lack of significance of the length in explaining the variation in the load cell readings was also anticipated since the moment capacities of beams of differing cross-sectional areas are not closely related to the lengths.

The amount of moment present for a given loading is however dependent on the length of the beam. Therefore, for beams with the same cross-sectional area, but of different length, the load cell readings would be expected to decrease as length increased.

However, the significant $A \times L$ interaction indicates clearly that the effect of beam length is not the same for 0.71 x 1.41-in. beams as it is for 1 x 2-in. beams. This is evident by the fact that with increasing beam length, the differences in load cell readings for beams of different cross-section become smaller. At lesser lengths, the load cell readings diverge reflecting an increasingly greater effect of cross-sectional area for given length.

The physical properties of the 18 beams tested in flexure are shown in Table 8 along with the measured and theoretical moments. Beams 1-7-27 and 2-1-36 were remade since failure occurred outside the middle third due to insufficient external stirrups. The loads obtained for the remade specimens are marked by an asterisk. The theoretical failure moments were less than the measured ultimate moments in all but two cases. The 1 x 2-in. beams were closer to the predicted failure moments than the smaller beams. Figure 11 shows the crack patterns exhibited

TABLE 8

ULTIMATE FAILURE MOMENTS OF BEAMS TESTED IN FLEXURE

Beam No.	Cross-Section	Span, in.	P, %	Actual Load Cell Reading, lbs.	Theo. Load Cell Reading, lbs.	M _{act.} in-lbs.	M _{theo.} in-lbs.	M _{act.} / M _{theo.}
1-7-18	.71x1.41-in.	18	0.883	225	205.6	675	617	1.094
2-7-18	"	18	"	230	205.6	690	617	1.118
3-7-18	"	18	"	205	205.6	615	617	0.997
1-7-27*	"	27	"	165	137.1	742	617	1.202
2-7-27	"	27	"	175	137.1	788	617	1.277
3-7-27	"	27	"	140	137.1	630	617	1.021
1-7-36	"	36	"	110	102.8	660	617	1.070
2-7-36	"	36	"	105	102.8	630	617	1.021
3-7-36	"	36	"	100	102.8	600	617	0.972
1-1-18	1 x 2-in.	18	"	625	581.6	1,875	1,745	1.074
2-1-18	"	18	"	600	581.6	1,800	1,745	1.031
3-1-18	"	18	"	635	581.6	1,905	1,745	1.092
1-1-27	"	27	"	400	387.8	1,800	1,745	1.031
2-1-27	"	27	"	410	387.8	1,845	1,745	1.057
3-1-27	"	27	"	410	387.8	1,845	1,745	1.057
1-1-36	"	36	"	310	290.8	1,860	1,745	1.066
2-1-36*	"	36	"	280	290.8	1,680	1,745	0.963
3-1-36	"	36	"	305	290.8	1,830	1,745	1.049

*Remade since the failure plane was located outside of the middle third. Results from replacement beam.



FIGURE 11. FLEXURE SPECIMENS AFTER FAILURE

by the beams tested. The flexure beams demonstrated the expected tension crack between the two load points.

Figure 12 is a graph of the average load cell reading versus the span length. The plot demonstrates the existence of significant interaction since the difference in results, for the two cross-sections, are not the same for each of the three span lengths.

In comparing the differences between the predicted load cell reading by Whitney's method and the average load cell reading from the flexure tests, a two-tailed "t" test was performed. The value of t being calculated from the formula

$$t = \frac{\bar{x} - \mu_0}{s} \sqrt{N} \quad (8)$$

where \bar{x} = average of the load cell readings from flexure tests in lbs.,

μ_0 = theoretical load cell reading computed by Whitney's method in lbs.,

s = standard deviation for individual observations,

and

N = 3, the number of specimens in each cell.

The computed value of t is shown in Table 9. For a probability level of 5 percent, t becomes significant when it is greater than 4.303. Only the results in cell 2-1-27 are significantly different from the predicted results computed by Whitney's method.

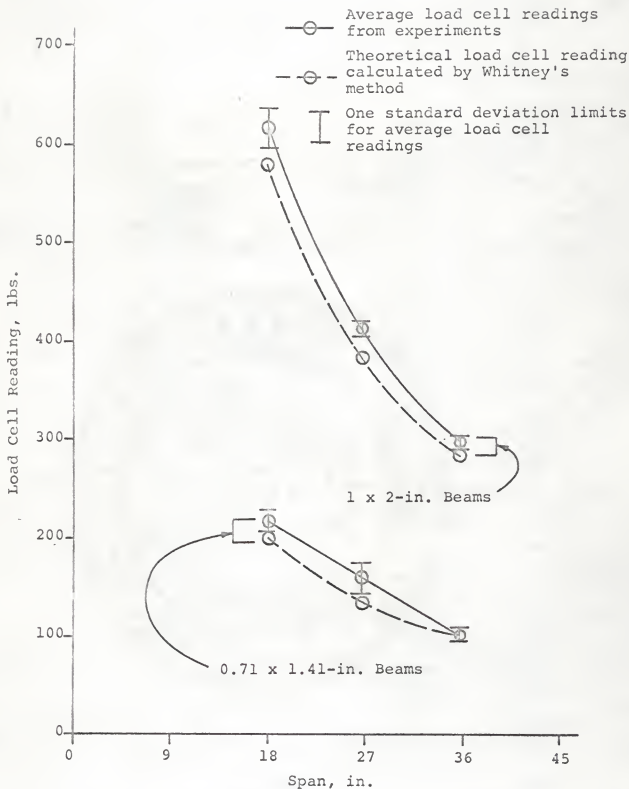


FIGURE 12. PLOT OF LOAD CELL READINGS VERSUS SPAN LENGTH FOR FLEXURE SPECIMENS

TABLE 9

STUDENT'S T-TEST FOR SIGNIFICANT DIFFERENCES BETWEEN
OBSERVED AND CALCULATED RESULTS FOR FLEXURE SPECIMENS

Cross Section		L		
		18	27	36
0.71 x 1.41-in.	μ_o	205.6	137.1	102.8
	\bar{x}	220.0	160.0	105.0
	s	13.23	18.03	5.00
	N	3	3	3
	t_{calc}	1.88	2.20	0.74
	$t_\alpha = .05$	4.30	4.30	4.30
	Sign.	No	No	No
1 x 2-in.	μ_o	581.6	387.8	290.8
	\bar{x}	620.0	406.7	298.3
	s	17.92	5.79	16.09
	N	3	3	3
	t_{calc}	3.71	5.65	2.64
	$t_\alpha = .05$	4.30	4.30	4.30
	Sign.	No	Yes	No

Conclusions Based on Flexure Experiment

The quality control samples exhibited consistent physical properties as shown by the analysis of variance for the compression and modulus of rupture specimens. The insignificant value of the F-ratios indicate this fact and allowed the 18 flexure specimens, cast from separate batches, to be considered as if they were from the same batch.

The results of the flexure experiments demonstrated consistent results as shown by the analysis of variance of the load cell readings. The two-way analysis of variance shown in Table 7, and the graph in Figure 12 demonstrate the significance of cross-section and span, and of interaction between the cross-section and span.

The Student's t-test showed that there was no significant difference between the mean value of the actual failure load for each cross-section-span combination and the calculated value of failure load for an alpha level of 5 percent with the exception of the beams in cell 1-27. The 0.71 x 1.41-in. beams were closer to the predicted load as demonstrated by the lower value of t_{calc} in the t-test. These results show that Whitney's method for predicting the ultimate strength of a beam in pure flexure is satisfactory.

TORSION TESTING PROGRAM

Review of Lessig's Theory

In 1959 Lessig developed a method for calculating the ultimate strength of a reinforced concrete beam in combined flexure and torsion. According to Lessig, a beam subjected to combined bending and torsion can fail in one of two modes. In the first mode the inclined neutral axis intersects the two vertical sides of the member which would indicate a high flexure to torsion ratio. For a low flexure to torsion ratio, the beam would fail in the second mode where the inclined neutral axis intersects the two horizontal surfaces of the beam as previously shown in Figure 13. Only the second mode of failure will be presented since only torsion is under consideration. The assumptions necessary to develop Lessig's theory are as follows:

- (1) The longitudinal and transverse reinforcing steel which crosses the tension cracks reaches its yield point at failure.
- (2) The tension capacity of the concrete is neglected.
- (3) The transverse reinforcement is uniformly spaced throughout the test section.
- (4) No external loads are applied within the test section.

Referring to Figure 13, for pure torsion

$$M_b = 0 \quad \text{and} \quad V = 0.$$

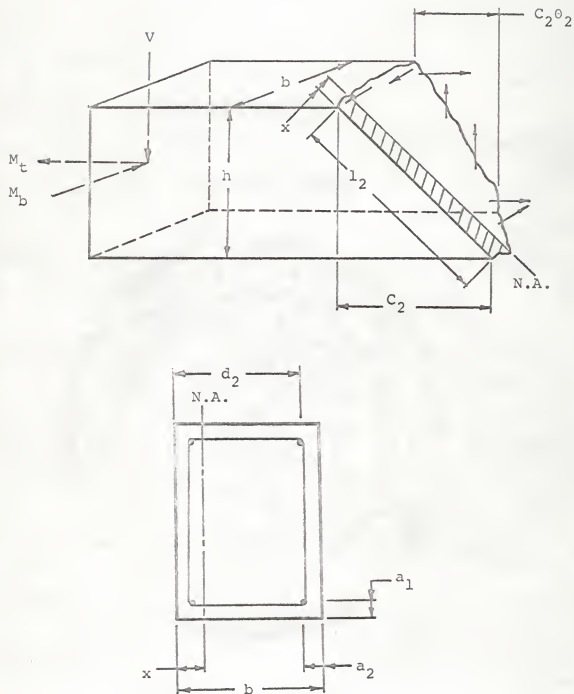


FIGURE 13. FREE BODY OF A RECTANGULAR REINFORCED CONCRETE BEAM UNDER COMBINED BENDING AND TORSION

The value of the external torsional moment vector along the neutral axis is given by

$$M_E = \frac{C_2}{l_2} M_{\text{theo}}.$$

The internal resisting moment consists of four parts.

1. Due to compression in the concrete, Figure 14.

$$M_1 = \int_0^{\rho} f_c'' \xi \frac{\xi}{2} \left(\frac{\rho}{l_2}\right) dy,$$

or

$$M_1 = \frac{f_c''}{2l_2} \int_0^{\rho} \xi^2 dy .$$

Then

$$\xi = x_1 + \left(\frac{x_2 - x_1}{\rho}\right)y .$$

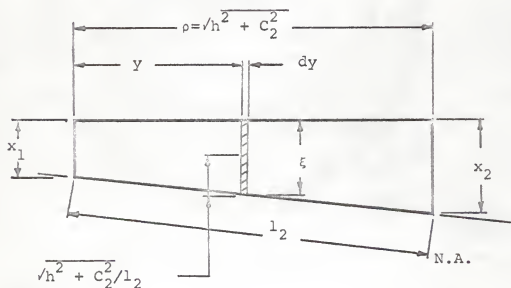


FIGURE 14. COMPRESSION ZONE AT FAILURE OF A RECTANGULAR REINFORCED BEAM

Therefore

$$M_1 = \frac{\rho f_c''}{2l_2} \int_0^{\rho} [x_1 + (\frac{x_2 - x_1}{\rho})y]^2 dy$$

or

$$M_1 = \frac{\rho f_c''}{2l_2} \int_0^{\rho} [x_1^2 + 2 \frac{(x_1 x_2 - x_1^2)}{\rho} y + \frac{(x_2 - x_1)^2}{\rho^2} y^2] dy .$$

Then

$$M_1 = \frac{\rho f_c''}{2l_2} [x_1^2 \rho + (x_1 x_2 - x_1^2) \rho + \frac{(x_2 - x_1)^2}{3} \rho]$$

or

$$M_1 = \frac{\rho^2 f_c''}{6l_2} (x_2^2 + x_1 x_2 + x_1^2) .$$

Finally

$$M_1 = \frac{(h^2 + C_2^2)}{6l_2} f_c'' (x_2^2 + x_2 x_1 + x_1^2) . \quad (9)$$

2. Due to the longitudinal steel.

$$M_2 = A_s f_y [d_2 - \frac{(x_1 + x_2)}{2}] \frac{h}{l_2} . \quad (10)$$

3. Due to the horizontal branch of the stirrups.

$$\text{Let } \cot \alpha = \frac{\frac{(C_2 - \theta_2 C_2)}{2}}{(b - \frac{x_1 + x_2}{2})} ,$$

$$\text{or } \cot \alpha = \frac{(1 - \theta_2)C_2}{2b - (x_1 + x_2)} .$$

Then

$$M_3 = A_v f_{vy} \frac{(b - x_1) \cot \alpha}{s} \left[\frac{(b - x_1) \cot \alpha}{2} \left(\frac{h}{C_2}\right) - a_1 \right] \frac{C_2}{l_2} \\ + A_v f_{vy} \frac{(b - x_2) \cot \alpha}{s} \left[\frac{(b - x_1) \cot \alpha}{2} \left(\frac{h}{C_2}\right) - a_1 \right] \frac{C_2}{l_2} .$$

Substituting the value for $\cot \alpha$ gives

$$M_3 = A_v f_{vy} \frac{(1-\theta_2)C_2^2}{s l_2} \left\{ \frac{h}{2}(1-\theta_2) \frac{(b-x_1)^2 + (b-x_2)^2}{[2b - (x_1+x_2)]^2} - a_1 \right\} . \quad (11)$$

4. Due to the vertical leg of the stirrups.

$$M_4 = \frac{C_2 \theta_2}{s} A_v f_{vy} \left[b - a_2 - \frac{(x_1 + x_2)}{2} \right] \frac{C_2}{l_2} \quad (12)$$

Equating the internal and external moments

$$\frac{C_2}{l_2} M_{\text{theo}} = M_1 + M_2 + M_3 + M_4 \quad (13)$$

$$\frac{C_2}{l_2} M_{\text{theo}} = \frac{(b^2 + C_2^2)}{6l_2^2} f_c'' (x_2^2 + x_2 x_1 + x_1^2) \\ + A_s f_y \left[d_2 - \frac{(x_1 + x_2)}{2} \right] \frac{h}{l_2} \\ + A_v f_{vy} \frac{(1-\theta_2)C_2^2}{s l_2} \left[\frac{h}{2}(1-\theta_2) \frac{(b-x_1)^2 + (b-x_2)^2}{(2b-x_1-x_2)^2} - a_1 \right] \\ + A_v f_{vy} \frac{C_2 \theta_2}{s} \left[b - a_2 - \frac{(x_1 + x_2)}{2} \right] \frac{C_2}{l_2} . \quad (14)$$

From equation (13), it can be seen that the internal moment depends only upon the values of x_1 , x_2 , C_2 and θ_2 .

The values of x_1 and x_2 must be such that the internal resisting moment is a minimum. Differentiating equation (14) with respect to x_1 and then x_2 yields identical results if $x_1 = x_2$. Therefore, it is necessary that $x_1 = x_2$. Substituting x for x_1 and x_2 into equation (14) gives

$$\begin{aligned} \frac{C_2}{I_2} M_{\text{theo}} &= \frac{(h^2 + C_2^2)}{2I_2} f_c'' x^2 + A_s f_y (d_2 - x) \frac{h}{I_2} \\ &+ A_v f_{vy} \frac{(1 - \theta_2) C_2^2}{S I_2} \left[\frac{h}{4} (1 - \theta_2) - a_1 \right] \\ &+ A_v f_{vy} \frac{\theta_2 C_2^2}{S} (b - a_2 - x) \frac{C_2}{I_2} . \end{aligned} \quad (15)$$

Differentiating equation (15) with respect to x yields

$$f_c'' x \frac{(h^2 + C_2^2)}{I_2} - A_s f_y \frac{h}{I_2} - A_v f_{vy} \frac{\theta_2 C_2^2}{S I_2} = 0.$$

Therefore

$$x = \frac{A_s f_y h + A_v f_{vy} (C_2/S) \theta_2}{f_c'' (h^2 + C_2^2)} . \quad (16)$$

If the tension crack has the same angle of inclination on all sides of the beam, the value of θ_2 will be

$$\theta_2 = \frac{h}{2b + h} \quad (17)$$

Since the maximum angle of the tension crack should be 45° the maximum value of C_2 is

$$C_2 = 2b + h. \quad (18)$$

Let

$$m = \frac{A_v f_{vy} b}{A_s f_y S} ,$$

$$\bar{\Delta}_1 = d_2 - \frac{x}{2} ,$$

and

$$\bar{\Delta}_2 = \theta_2 (b - a_2 - \frac{x}{2}) + \frac{h}{4} (1 - \theta_2)^2 - a_1 (1 - \theta_2) .$$

Then

$$M_{\text{theo}} = A_s f_y \frac{h}{C_2} (\bar{\Delta}_1 + \bar{\Delta}_2 \frac{m C_2^2}{b y}) . \quad (19)$$

From equation (19) the theoretical torsional capacity can be calculated for a given cross-section. For evaluating the test specimens, the value of θ_2 and C_2 should be measured from the actual crack pattern at failure. The expressions $\theta_2 C_2 / S$ in equation (16) and $[(b-x)/S] \cot \alpha$ in equation (11) are the theoretical number of stirrups which intersect the failure surface. The actual number of stirrups should be used in analyzing the test specimens.

Making the necessary substitutions to analyze the test specimens yields the four moment components as:

$$M_1 = f_c x^2 \frac{(h^2 + C_2^2)}{2 I_2} ,$$

$$M_2 = A_s f_y (d_2 - x) \frac{h}{I_2} ,$$

$$M_3 = A_v f_{vy} N_h \left[\frac{C_2 (1 - \theta_2) h}{4 C_2} - a_1 \right] \frac{C_2}{I_2} ,$$

and

$$M_4 = A_v f_{vy} N_v (b - a_2 - x) \frac{C_2}{l_2} .$$

Let

N_v = number of the vertical branches of the stirrups intersecting the tension crack

and

N_h = number of the horizontal branches of the stirrups intersecting the tension crack.

From equation (13),

$$\begin{aligned} M_{\text{calc}} \left(\frac{C_2}{l_2} \right) &= M_1 + M_2 + M_3 + M_4 \\ &= f_c'' x^2 \frac{(h^2 + C_2^2)}{2l_2} + A_s f_y (d_2 - \frac{x}{2}) \frac{h}{l_2} \\ &\quad + A_v f_{vy} N_h \left[\frac{(1 - \theta_2)h}{4} - a_1 \right] \frac{C_2}{l_2} \\ &\quad + A_v f_{vy} N_v (b - a_2 - x) \frac{C_2}{l_2} . \end{aligned} \quad (20)$$

Since

$$\frac{\delta M_{\text{calc}}}{\delta x} = 0 = f_c'' x \frac{(h^2 + C_2^2)}{l_2} - A_v f_{vy} N_v \frac{C_2}{l_2} - A_s f_y \frac{h}{l_2}$$

which yields

$$x = \frac{h A_s f_y + A_v f_{vy} C_2 N_v}{f_c'' (h^2 + C_2^2)} . \quad (21)$$

Substituting this value of x into equation (20) gives

$$M_{\text{calc}} = A_s f_y \left(\frac{h}{C_2}\right) \left(d_2 - \frac{x}{2}\right) + A_v f_{vy} N_v (b - a_2 - \frac{x}{2}) + A_v f_{vy} N_h \left[\frac{(1 - \theta_2)h}{4} - a_1\right]. \quad (22)$$

Let

$$m = \frac{A_v f_{vy} b}{A_s f_y S}, \quad (23)$$

$$\Delta_1 = d_2 - \frac{x}{2}, \quad (24)$$

and

$$\Delta_2 = N_v (b - a_2 - \frac{x}{2}) + N_h \left[\frac{h}{4}(1 - \theta_2) - a_1\right]. \quad (25)$$

This gives the internal torsional capacity of the cross-section using the measured values C_2 , θ_2 , N_v , and N_h as

$$M_{\text{calc}} = A_s f_y \frac{h}{C_2} \left(\Delta_1 + \Delta_2 \frac{m C_2 S}{hb}\right). \quad (26)$$

The torsional moment computed on this basis, M_{meas} , is computed using the actual measured parameters of the specimen. The applied torsional moment is referred to as M_{act} .

Lessig suggests that for a tension failure, a reasonable value of m must be used when designing the beams. For a balanced section the ratio of transverse force to longitudinal force in the reinforcing steel would be 1.0. From the previous tests by Lessig, good results were obtained when m ranged between 0.3 to 1.0. Cardenas (7) also obtained reasonably good results for values of m from 0.4 to 0.7.

If a compression failure occurs, equation (26) gives a much higher value for the measured and theoretical moments. Therefore, for compression failures Lessig suggests the use of the empirical formula

$$M_c = kb^2hf'_c \quad , \quad (27)$$

where k is a constant determined by Lessig to range from 0.07 to 0.12.

Timoshenko (6) in 1949 suggested that the elastic torque could be computed according to the formula

$$M_{el} = f'_t \varnothing b^2 h \quad , \quad (28)$$

where \varnothing is a function of h and b . When $h/b = 2$, $\varnothing = 0.246$.

According to the plastic theory, the torque at failure is given by

$$M_p = f'_t b^2 (3h - b) \frac{1}{6} \quad . \quad (29)$$

Design of Experiment for Torsion Tests

The experimental program consisted of testing 18 beams in pure torsion. The beams were of two sizes, namely 1 x 2-in. and 1.41 x 2.83-in. Three values of m , the ratio of transverse force to longitudinal force in the reinforcing steel, were selected for each cross-section. These were: 0.4, 0.5, and 0.6. Three specimens were fabricated for each cross-sectional area - m combination. The beams were designed to induce yielding of the reinforcement as the mode of failure in torsion. The percentage

of longitudinal reinforcement was constant while the amount of transverse reinforcement was varied to give the required values of m . The experimental design is shown in Table 10.

TABLE 10
DESIGN OF EXPERIMENT FOR TORSION TESTS

Cross Section	m		
	0.4	0.5	0.6
1 x 2-in.	1	1	1
	2	2	2
	3	3	3
1.41 x 2.83-in.	1	1	1
	2	2	2
	3	3	3

Results from Quality Control Tests

For each torsion specimen tested four quality control samples were cast. Two were tested in compression and two in flexure. The results for quality control are shown in Table 11, for compressive strength, and in Table 12, for modulus of rupture. The upper and lower compressive strength values for individual batch means, shown at the bottom of Table 11, are 2,709 psi. and 2907 psi. The average compressive strength values for

the 18 batches range from 2715 psi. to 2895 psi. which are within the range of values for upper and lower compressive strength required for the assumption that the values obtained are no different than those that would have been obtained from 18 test specimens from a single batch for an alpha probability level of 0.05.

A comparison of upper and lower values of modulus of rupture, for individual batches, with average values for the 18 batches, Table 12, leads to the same assumption as that for compressive strength. That is, all 18 batches can be assumed to yield modulus of rupture results which are no different than the results that would have been obtained if all test specimens had come from the same batch. These assumptions are further born out in the Analysis of Variance computations shown in Table 13, where batch-to-batch differences cannot be differentiated from within-batch differences when tested at the alpha level of 0.05.

Procedures Used in the Torsion Tests

The two cross-sections tested are shown in Figure 15. The numbering system used when referring to the torsion specimens is the same as that used in the flexure tests except for the torsion specimens in which the third number refers to the value of m for that beam.

The testing apparatus used for the torsion specimens is shown in Figure 16. The cylinder holding the beam where the torque was applied was fabricated concentric with the shaft. The specimen was held in place using four cap screws and was

TABLE 11

COMPRESSIVE STRENGTH OF QUALITY CONTROL SAMPLES FOR TORSION BEAMS

		Compressive Strength, psi.																
Batch	1	2	3	4	5	6	7	8	9									
Beam	1-1-.4	2-1-.4	3-1-.4	1-1-.5	2-1-.5	3-1-.5	1-1-.6	2-1-.6	3-1-.6									
(1)	2,930	2,880	2,820	2,780	2,680	2,710	2,880	2,780	2,900									
(2)	<u>2,860</u>	<u>2,760</u>	<u>2,760</u>	<u>2,830</u>	<u>2,750</u>	<u>2,780</u>	<u>2,850</u>	<u>2,840</u>	<u>2,850</u>									
Average	2,895	2,820	<u>2,790</u>	<u>2,805</u>	<u>2,715</u>	<u>2,745</u>	<u>2,865</u>	<u>2,810</u>	<u>2,875</u>									
Batch	10	11	12	13	14	15	16	17	18									
Beam	1-1.4-.4	2-1.4-.4	3-1.4-.4	1-1.4-.5	2-1.4-.5	3-1.4-.5	1-1.4-.6	2-1.4-.6	3-1.4-.6									
(1)	2,840	2,810	2,760	2,860	2,820	2,790	2,750	2,800	2,830									
(2)	<u>2,790</u>	<u>2,880</u>	<u>2,810</u>	<u>2,790</u>	<u>2,900</u>	<u>2,720</u>	<u>2,840</u>	<u>2,720</u>	<u>2,770</u>									
Average	2,815	2,845	<u>2,785</u>	<u>2,825</u>	<u>2,860</u>	<u>2,755</u>	<u>2,795</u>	<u>2,760</u>	<u>2,800</u>									

Lower Confidence Limit for batch means = 2,709 psi.

Upper Confidence Limit for batch means = 2,907 psi.

TABLE 12

MODULUS OF RUPTURE OF QUALITY CONTROL SAMPLES FOR TORSION BEAMS

		Modulus of Rupture, psi.									
		1	2	3	4	5	6	7	8	9	
Batch	1-1-.4	402	414	402	414	452	389	377	402	414	
Beam	1-1-.4	439	377	427	427	414	414	427	439	377	
	(1)	421	396	415	421	433	402	402	421	396	
	(2)										
Average											
Batch	1-1.4-.4	439	377	427	402	414	452	439	377	439	
Beam	1-1.4-.4	427	414	389	439	377	414	414	427	389	
	(1)	433	396	407	421	396	433	427	402	414	
	(2)										
Average											
Batch	1-1.4-.4	439	377	427	402	414	452	439	377	439	
Beam	1-1.4-.4	427	414	389	439	377	414	414	427	389	
	(1)	433	396	407	421	396	433	427	402	414	
	(2)										
Average											

Lower Confidence Limit for batch means = 386 psi.

Upper Confidence Limit for batch means = 444 psi.

TABLE 13

ANALYSIS OF VARIANCE TABLES FOR QUALITY CONTROL SAMPLES FOR TORSION SPECIMENS

(a) Analysis of Variance Tables for Compression Samples

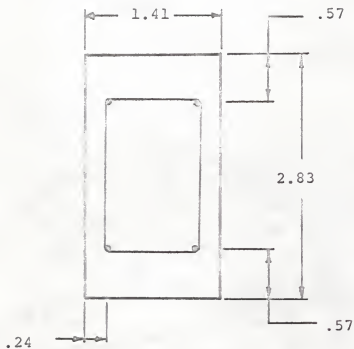
Source	Degrees of Freedom	Sum of Squares	Mean Squares	Table		Significance
				F Test	$\alpha = .05$	
Between	17	65,740	3,867	1.66	2.23	No
Within	18	41,700	2,317			
Total	35	107,440				

Coefficient of Variation = 1.97 percent Grand Average = 2,808 psi.

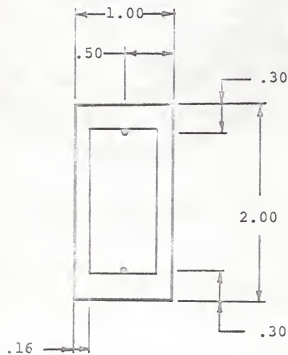
(b) Analysis of Variance Table for Modulus of Rupture Samples

Source	Degrees of Freedom	Sum of Squares	Mean Squares	Table		Significance
				F Test	$\alpha = .05$	
Between	17	6,640	390.6	0.60	2.23	No
Within	18	11,670	648.3			
Total	35	18,310				

Coefficient of Variation = 5.51 percent Grand Average = 415 psi.



(a) Typical Cross-section of 1.41 x 2.83-in. Beam



(b) Typical Cross-section of 1 x 2-in. Beam

FIGURE 15. TYPICAL CROSS-SECTION OF TORSION SPECIMENS



FIGURE 16. TORSION SPECIMEN IN TESTING APPARATUS

centered by counting the threads showing on the cap screws on the outside of the cylinder. The torque was applied through a 20 in. lever arm by a hydraulic jack.

The load cell was attached to the lever arm and the force from the jack was applied through the cell. The beam was placed in the testing apparatus so that the lever arm was approximately 15 degrees below horizontal. This procedure produced some error in measuring the initial load but as the specimen rotated the lever arm became more nearly horizontal, and consequently, the load was measured more accurately. Some difficulty was encountered with the load cell at the small loads measured since the maximum capacity of the cell was 50,000 lbs. whereas the loads being read were less than 100 lbs. After the specimens failed, a zero reading was taken and the necessary correction for zeroing the cell was added or subtracted.

The rotation of the specimens tested in torsion was measured by the use of two slide projectors and two mirrors which were attached to the beams one foot apart. The images of the mirrors were projected onto two scales 11.40 ft. from the beam. After each 5 lbs. loading increment, the movements of the images of the mirrors was noted and the unit angle of twist was calculated by the formula

$$\gamma = \frac{\Delta_L - \Delta_R}{DR} \quad (30)$$

where

Δ_L = the change in the left scale reading after a load increment in ft.,

Δ_R = the change in the right scale reading after a load increment in ft.,

D = the gage length between the center line of the two mirrors in ft.,

and

R = the distance between the specimen and the scales in ft.

Although this does not give the exact rotation, equation (30) allows approximate torque-twist curves to be plotted. These curves are shown in Appendix A.

Analysis of Results from Torsion Experiment

The ultimate load cell readings are shown in Table 14 for the reinforced beams tested in torsion. An analysis of variance was performed on the load cell readings and is also shown in Table 14. This analysis shows that the difference in cross-sectional area, A, accounts for a significant part of the variation in ultimate load cell reading. This was anticipated since the torque carrying capacity of a beam is, according to Lessig, approximately proportional to the linear dimensions of the cross-section. The lack of significance of the m ratio, when summing across areas, was also anticipated since its effect is almost identical with that of the length in the flexure tests. That is, within an area grouping m should have been quite significant in explaining variation in the data, but across cross-sectional it would lose its significance. This should

have resulted in m not being significant and in $A \times m$ being significant. However an examination of the data in Table 14 immediately indicates that m had no significance even within area groupings. The average load cell reading, standard deviation, and coefficient of variation is also given in Table 14 for each cross-sectional area- m combination. Only the 1 x 2-in. with $m = 0.5$ had a coefficient of variation less than 5 percent.

The physical properties of the 18 beams tested are shown in Table 15 with the measured, calculated, and theoretical moments where

M_{meas} = actual failure moment determined from load cell readings in ft-lbs.,

M_{calc} = moment calculated by Lessig's theory using the measured parameters, C_2 , $C_2\theta_2$, N_v , and N_h in in-lbs.,

and M_{theo} = moment calculated by Lessig's theory using calculated parameters C_2 and $C_2\theta_2$ in in-lbs.

The measured torsional moments were greater than the calculated moments but less than the theoretical moments for the 1 x 2-in. beams. For the larger beams the measured failure torques were approximately half of the calculated moments but only about one-third of the theoretical moments.

The crack patterns exhibited by the torsion specimens are shown in Figure 17. According to Lessig, the failure of the beam should take the form of helical cracks at approximately

TABLE 14
ANALYSIS OF ULTIMATE LOAD CELL READINGS OF TORSION BEAMS

Cross Section	m		
	0.4	0.5	0.6
	Ultimate Load Cell Readings		
1 x 2-in.	32	32*	24*
	24*	30	30*
	<u>37*</u>	<u>33*</u>	<u>39</u>
Average	31	32	31
Standard Deviation	6.56	2.24	7.55
Coefficient of Variation	21.20	1.58	24.35
1.41 x 2.83-in.	34	44	46*
	44	42*	47
	<u>44</u>	<u>39*</u>	<u>40*</u>
Average	41	42	44
Standard Deviation	5.79	2.55	3.81
Coefficient of Variation	14.24	6.12	8.59

(continued on next page)

TABLE 14
 ANALYSIS OF ULTIMATE LOAD CELL READINGS OF TORSION BEAMS
 (continued)

Source	df	SS	MS	F	F $\alpha = .05$	Sign.
Cross Section, A	1	545	545.0	90.83	18.50	Yes
Ratio, m	2	10	5.0	0.83	19.00	No
A x m	2	12	6.0	0.23	3.89	No
Spec. in A x m cells	12	313	26.1			
Total	17	880				

*Measured value of C_2 obtained by adding twice the horizontal length of the bottom crack.

TABLE 15

MEASURED PARAMETERS AND CALCULATED MOMENTS FOR TORSION SPECIMENS

Beam No.	m	P %	Measured				θ_2	M_{meas} in-lbs	M_{calc} in-lbs	M_{theo} in-lbs	$\frac{M_{\text{theo}}}{M_{\text{meas}}}$	$\frac{M_{\text{calc}}}{M_{\text{meas}}}$	$\frac{M_{\text{theo}}}{M_{\text{calc}}}$
			C_2 in.	$C_2^{\theta_2}$ in.	N_V	N_h							
1-1-0.4	0.40	0.83	3.69	2.19	2	2	0.594	640	494	655	1.300	0.978	0.755
2-1-0.4*	0.40	0.83	3.50	1.75	2	2	0.500	480	478	655	1.002	0.733	0.731
3-1-0.4*	0.40	0.83	3.88	1.38	2	2	0.356	700	468	655	1.580	1.130	0.715
1-1-0.5*	0.50	0.83	4.00	2.25	3	2	0.562	640	524	760	1.221	0.833	0.690
2-1-0.5	0.50	0.83	3.81	1.38	2	2	0.362	600	466	760	1.288	0.790	0.606
3-1-0.5*	0.50	0.83	3.88	1.88	3	2	0.485	660	527	760	1.252	0.869	0.694
1-1-0.6*	0.60	0.83	3.75	2.00	4	3	0.532	480	606	868	0.792	0.553	0.698
2-1-0.6*	0.60	0.83	3.56	1.56	3	3	0.438	600	551	868	1.089	0.691	0.635
3-1-0.6	0.60	0.83	3.94	1.88	3	3	0.477	780	523	868	1.493	0.899	0.602
1-1.4-0.4	0.40	0.83	5.12	3.00	2	2	0.585	680	1288	2,330	0.528	0.295	0.553
2-1.4-0.4	0.40	0.83	5.50	3.25	2	2	0.590	880	1241	2,330	0.710	0.378	0.533
3-1.4-0.4	0.40	0.83	4.75	2.50	1	2	0.526	880	1122	2,330	0.785	0.378	0.481
1-1.4-0.5	0.50	0.83	4.50	2.25	1	2	0.500	880	1170	2,545	0.745	0.347	0.460
2-1.4-0.5*	0.50	0.83	4.62	2.62	1	2	0.568	840	1147	2,545	0.733	0.330	0.451
3-1.4-0.5*	0.50	0.83	5.38	3.75	2	2	0.698	780	1256	2,545	0.622	0.306	0.493
1-1.4-0.6*	0.60	0.83	6.00	3.00	2	2	0.500	920	1180	2,760	0.780	0.334	0.427
2-1.4-0.6	0.60	0.83	5.18	2.50	2	2	0.786	940	1285	2,760	0.685	0.330	0.466
3-1.4-0.6*	0.60	0.83	5.75	3.00	2	2	0.522	800	1209	2,760	0.729	0.290	0.438

*Measured value of C_2 obtained by adding twice the horizontal projection of the bottom crack to $C_2^{\theta_2}$.



FIGURE 17. CRACK PATTERNS OF TORSION SPECIMENS

45 degrees with the longitudinal axis of the beam. Since the complete length of the specimen is under the same torque, the cracks should start at random locations. This was not the case however, in this study. The tension cracks in the 1 x 2-in. beams generally started at the pinned support and worked across the beam. For the larger beams, the tension cracks usually started at the support where the torque was applied. In some cases a crack pattern of sufficient length to measure the value of C_2 was not developed. That is, the tension crack failed to make one complete revolution around the specimen. These beams are marked in Table 15 by an asterisk. To obtain the required value of C_2 , twice the horizontal projection of the crack on the bottom of the beam was added to $C_2^{\theta_2}$, the horizontal projection of the crack along the side of the beam.

Using the elastic theory presented by Timoshenko, the moments predicted for the 1 x 2-in. and 1.41 x 2.83-in. beams respectively are

$$M_{e1} = 204 \text{ in-lbs. and } M_{e1} = 980 \text{ in-lbs.}$$

The above values were calculated using the value of f'_t obtained from the analysis of variance of the control samples.

Figure 18 shows the average experimental, calculated, and theoretical load cell readings versus m . The curves illustrate graphically the wide divergence of the results for the larger beams. The results for the smaller beams are in much closer agreement.

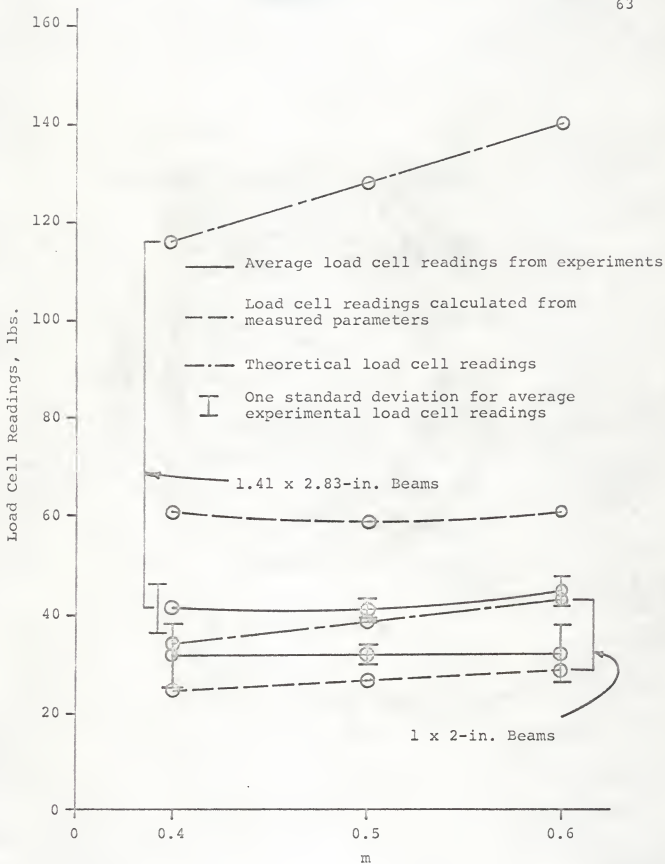


FIGURE 18. PLOT OF LOAD CELL READINGS VERSUS m FOR TORSION SPECIMENS

For the analysis of the test results, the values of M_{calc} and M_{theo} were reduced to a theoretical load cell reading by dividing the moment by the 20 in. lever arm. According to Lessig's torsion theory, M_{calc} and M_{theo} should be the same. To test the difference between the measured, calculated, and theoretical load cell readings, the Student's t-test was performed. Table 16 gives the comparison using the average M_{calc} as the theoretical value of the mean, μ_0 . For an $\alpha = 0.05$, the assumed hypothesis that the mean of M_{calc} and M_{meas} are the same would be accepted for all of the 1 x 2-in. beams but rejected for all of the 1.41 x 2.83-in. beams. Table 17 gives the Student's t-test with M_{theo} as the theoretical value of the mean. For an $\alpha = 0.05$, the hypothesis would be accepted only for values of m of 0.4 and 0.5 for the 1 x 2-in. beams.

As expected, the slope of the linear portion of the torque-twist curves for the 1 x 2-in. beams was generally less than that for the 1.41 x 2.83-in. specimens. (Appendix A). It was further expected that the specimens would continue to take load after the initial tension cracks started but this was not the case. In every specimen tested, the load dropped off immediately at initial cracking and continued to drop until ultimate failure occurred.

Conclusions Based on Torsion Experiment

The quality control samples exhibited acceptable uniformity and allowed the assumption that batch-to-batch differences could be ignored when analyzing the test data.

TABLE 16

STUDENT'S T-TEST FOR SIGNIFICANT DIFFERENCES
BETWEEN M_{meas} AND M_{calc} FOR TORSION SPECIMENS

Cross Section		m		
		0.4	0.5	0.6
1 x 2-in.	μ_0	24.0	25.3	28.0
	\bar{x}	31.0	31.7	31.0
	s	6.56	2.24	7.55
	N	3	3	3
	t_{calc}	1.85	4.95	0.69
	$t_\alpha = .05$	4.30	4.30	4.30
	Sign.	No	Yes	No
1.41 x 2.83-in.	μ_0	60.8	59.6	61.2
	\bar{x}	40.7	41.7	44.3
	s	5.79	2.55	3.81
	N	3	3	3
	t_{calc}	6.02	12.18	7.69
	$t_\alpha = .05$	4.30	4.30	4.30
	Sign.	Yes	Yes	Yes

TABLE 17

STUDENT'S T-TEST FOR SIGNIFICANT DIFFERENCES
 BETWEEN M_{meas} and M_{theo} FOR TORSION SPECIMENS

Cross Section		m		
		0.4	0.5	0.6
1 x 2-in.	μ_0	32.8	38.0	43.4
	\bar{x}	31.0	31.7	31.0
	s	6.56	2.24	7.55
	N	3	3	3
	t_{calc}	0.48	4.87	2.84
	$t_\alpha = .05$	4.30	4.30	4.30
	Sign.	No	Yes	No
1.41 x 2.83-in.	μ_0	116.5	127.2	138.0
	\bar{x}	40.7	41.7	44.3
	s	5.79	2.55	3.81
	N	3	3	3
	t_{calc}	22.60	58.10	42.60
	$t_\alpha = .05$	4.30	4.30	4.30
	Sign.	Yes	Yes	Yes

The analysis of variance of the ultimate load cell reading showed inconsistent results for all specimens tested except for those of cell 1-0.5. The two-way analysis of variance shown in Table 14 and the graph in Figure 18 showed the insignificance of the effect of m and of the interaction between m and A on the load cell readings. These parameters should be significant in the analysis as the ratio of transverse to longitudinal steel in the beam is important in determining its strength in torsion. The interaction between m and A should have been significant. No explanation is offered for this lack of agreement other than possible difficulties with the torsion test apparatus which, because of its crudeness, may not have been loading test specimens in the manner assumed.

The Student's t -test showed no significant difference between the mean value of the actual failure moment for the 1 x 2-in. beams using either M_{calc} or M_{theo} as the mean. The Student's t -test showed very significant differences between the measured moment and both the calculated and theoretical moments used as the mean for the 1.41 x 2.83-in. beams.

The significant differences between the mean and the measured moments could be due to a misalignment of the supports as a new fixture was used for the pinned end for the larger beams. The test apparatus only allowed for a check of vertical alignment using a level.

Lessig's theory did not predict the strength of the beams tested in torsion as shown by the t-tests. The spacing of the transverse reinforcement was varied in an attempt to produce significant differences in the ultimate strength of the beams but this did not occur. The torsion capacity of the 1.41 x 2.83-in. beams was not much greater than that of the smaller beams. This would indicate errors in the fabrication or testing of the beams.

GENERAL CONCLUSIONS

The Ultracal-30 mix used in the experiments was a satisfactory substitute for 3,000 psi. concrete in terms of compressive strength. The modulus of rupture of the 1 x 1 x 4-in. specimens was high when compared to that of 3,000 psi. concrete. The analysis of variance of the specimens used to design the mix and used to analyze the quality control samples demonstrated the insignificance of the batch-to-batch variance.

The flexural testing program indicated that small scale model testing could be used with confidence to predict the ultimate strength of beams loaded in flexure. In most cases the beams failed at loads slightly higher than those predicted by Whitney's theory.

The results of this study indicate that the values of the calculated and theoretical moments indicated by Lessig's theory for the 1 x 2-in. beams predicted the failure torque as shown in the Student's t-test. Lessig's theory failed to predict the ultimate torque for the larger beams as did the elastic and plastic theories.

RECOMMENDATIONS FOR FURTHER RESEARCH

The problem of flexure in rectangular under-reinforced sections has been thoroughly studied. However, a statistical approach has not been used to analyze the test results of concrete beams of other shapes. Work is needed in the area of model analysis of T-beams and box-section beams. Different sections of under-reinforced prestressed concrete beams also need investigation to determine if model analysis gives reasonable results.

Although the longitudinal reinforcing steel after annealing was satisfactory, the two types of smooth wire used as transverse reinforcement had many undesirable properties. The black annealed wire used in the smaller torsion specimens was extremely soft and exhibited a low yield point. While the bright basic wire used in the large torsion specimens was quite satisfactory, it could not be obtained in a smaller diameter. Wire with a yield point of 50 ksi. available in many diameters is badly needed. This would allow reasonable spacing of the stirrups.

For the flexure specimens the copper bar chairs were insufficient for holding the longitudinal reinforcement in place. A better method of supporting the reinforcing steel for beams containing internal stirrups is needed. Although extra bar chairs placed on top of the reinforcing steel helped, difficulty was experienced in alignment of the steel in the forms.

The results of this study indicate that definite limits need to be established concerning the ratio of longitudinal

reinforcement to concrete compressive strength. Lessig states that the torsion theory gives good results for an m of 0.4 to 1.0. Limits also need to be defined accurately for this ratio.

The testing apparatus used for the torsion experiment requires refinement to insure correct alignment of the specimen. The apparatus should be constructed so as to prevent an impact load being applied to the specimen when the concrete first cracks.

LIST OF SYMBOLS

a	= depth of the compression stress block in flexure beams, in.
A_s	= cross-sectional area of longitudinal steel, in. ²
A_v	= cross-sectional area of one leg of the stirrups, in. ²
b	= width of beam
c	= lever arm of internal forces in Whitney's method, in.
C_2	= total length of cracked surface projected along the longitudinal axis of beam, in.
d	= effective depth of beam, in.
D	= the gage length between the center line of the two mirrors
E	= modulus of elasticity, psi.
f_{vy}	= yield stress of transverse reinforcement, psi.
f_y	= yield stress of longitudinal reinforcement, psi.
f'_c	= concrete strength in compression, psi.
f''_c	= design strength of concrete, psi.
f'_t	= flexure strength of the concrete, psi.
h^t	= total depth of beam
L	= span of beam
m	= ratio of transverse to longitudinal force in the beam
M_b	= external bending moment, in-lbs.
M_{calc}	= moment calculated from measured parameters, in-lbs.

- M_{meas} = moment calculated from load cell readings, in-lbs.
 M_{el} = torque computed using the elastic theory, in-lbs.
 M_p = torque computed using the plastic theory, in-lbs.
 M_{theo} = moment calculated from theories, in-lbs.
 N = number of specimens in a cell
 N_h = number of horizontal branches of stirrups intersecting the failure surface
 N_v = number of vertical branches of stirrups intersecting the failure surface
 $p = \frac{A_s}{bd}$
 R = distance between the specimens and scales, ft.
 s = standard deviation
 S = stirrup spacing, in.
 $t = \text{computed by } \frac{\bar{x} - \mu_0}{s/\sqrt{N}}$ in the Student's t-test
 V = shear force, lbs.
 \bar{x} = mean of the samples in a cell
 x = depth of the compression zone in torsion, in.
 α = probability level of rejecting a true hypothesis
 Δ_L = change in left scale reading, ft.
 Δ_R = change in right scale reading, ft.
 μ_0 = theoretical value of the mean
 $\theta_2 C_2$ = projected length of crack on side opposite to the compression face of the specimen, in.

ACKNOWLEDGEMENTS

The author wishes to express his sincere appreciation to Dr. Robert R. Snell, his faculty advisor, under whose direction this study was carried out and to Dr. Jack B. Blackburn, Head of the Department of Civil Engineering, for his valuable advice in analyzing the results of this study.

Sincere thanks are due Messrs. S. K. Kapur, H. Kamil, J. S. Arora, and W. M. Lackey for their help in conducting the many tests.

BIBLIOGRAPHY

1. Winter, George. Design of Concrete Structures, Seventh Edition, McGraw-Hill, New York, 1964.
2. Onesti, D. "Investigation of Direct Small Scale Model Analysis of Reinforced Concrete Flexural Members," unpublished M.S. Thesis, Cornell University, Feb. 1964.
3. Lessig, N. N. "Determination of the Load-carrying Capacity of Reinforced Concrete Elements with Rectangular Cross-section Under Simultaneous Action of Flexure with Torsion," Benton i Zhelezobeton, No. 3, 1959, pp. 109-113. (Foreign Literature Study No. 348.)¹
4. Lessig, N. N. "Determination of the Load-carrying Capacity of Reinforced Concrete Elements with Rectangular Cross-section Subjected to Flexure with Torsion," No. 5, 1959, pp. 5-28. (Foreign Literature Study No. 371.)¹
5. Lessig, N. N. "Study of Cases of Failure of Concrete in Reinforced Concrete Elements with Rectangular Cross-section Subjected to Combined Flexure and Torsion," Design of Concrete Structures, State Publishing Office of Literature on Structural Engineering, Architecture, and Structural Materials, Moscow. (Foreign Literature Study No. 398.)¹
6. Fan, W. R. S. "Behavior of Reinforced Plaster Model Beams in Bending and in Torsion," Unpublished M.S. Thesis, University of North Carolina at Raleigh, 1964.
7. Cardenas, Raul. "A Study of Reinforced Plaster Model Beams in Combined Bending and Torsion," unpublished M.S. Thesis, University of North Carolina at Raleigh, 1965.
8. Burton, K. "A Technique Developed to Study the Ultimate Strength of Prestressed Concrete Structures by the Use of Small Scale Models," unpublished M.S. Thesis, Cornell University, Feb. 1964.
9. Chao, N.-P. "Ultimate Flexural Strength of Prestressed Concrete Beams by Small Scale Model Analysis," unpublished M.S. Thesis, Cornell University, Feb. 1964.

¹Translated from the Russian by Margaret Corbin for the Research and Development Library of the Portland Cement Association, Skokie, Illinois.

10. Hognestad, Eivind, Hanson, N. W., and McHenry, D. "Concrete Stress Distribution in Ultimate Strength Design," Journal, ACI Proc., Vol. 27, No. 4, Dec. 1955, p. 455.
11. White, Richard N. "Small Scale Models of Concrete Structures," presented at the ASCE Structural Engineering Conference and Annual Meeting, Conference Reprint 131, Oct. 19-23, 1964.

APPENDIX A

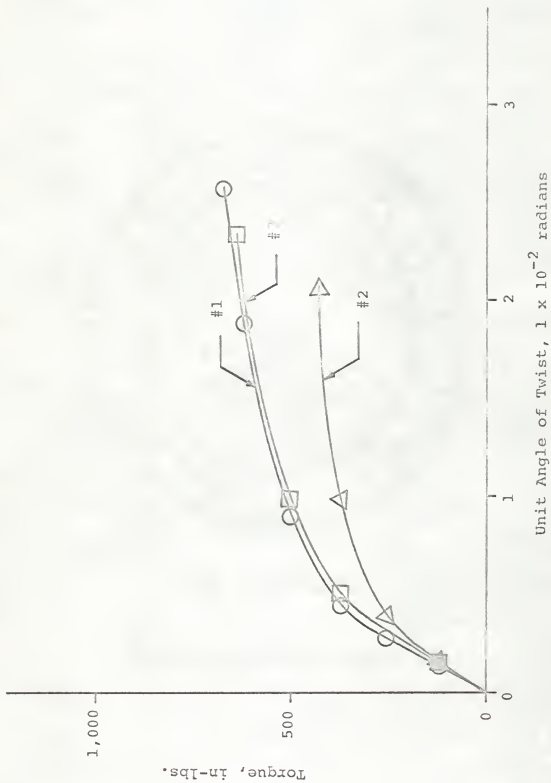
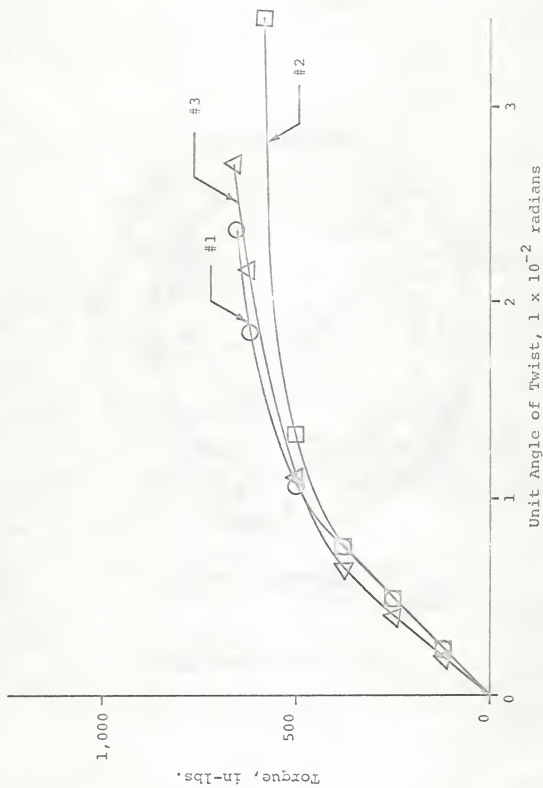


FIGURE 19. TORQUE-TWIST CURVES FOR BEAMS 1-0.4



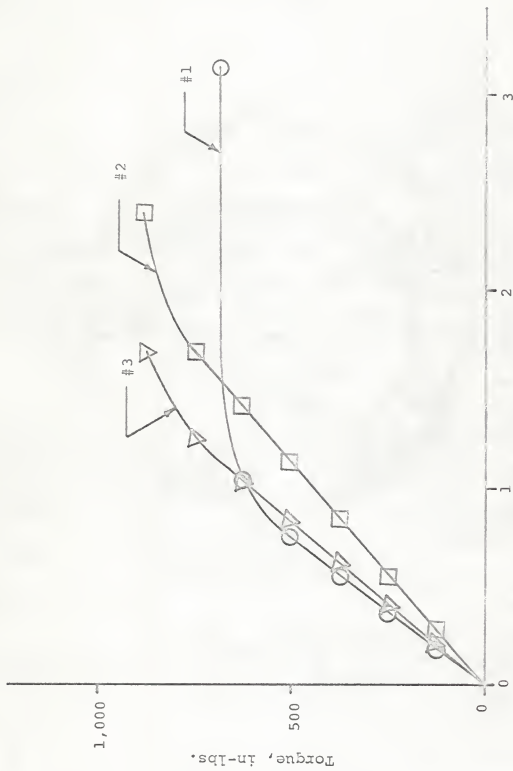
Unit Angle of Twist, 1×10^{-2} radians

FIGURE 20. TORQUE-TWIST CURVES FOR BEAMS 1-0.5



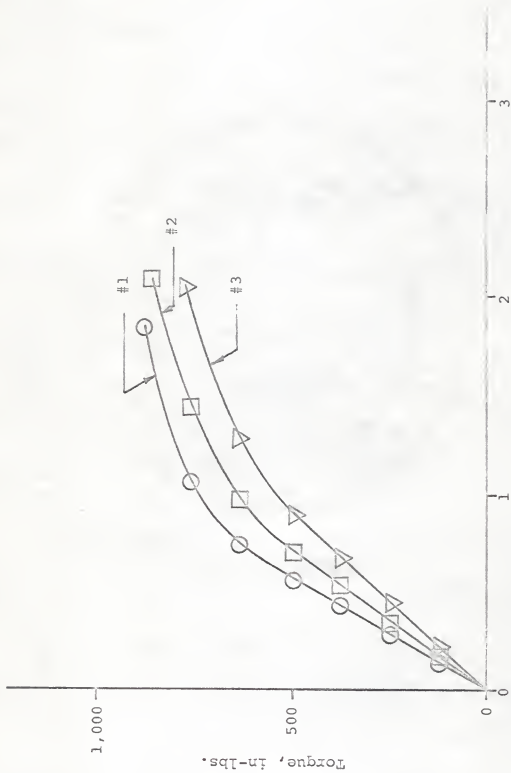
Unit Angle of Twist, 1×10^{-2} radians

FIGURE 21. TORQUE-TWIST CURVES FOR BEAMS 1-0.6



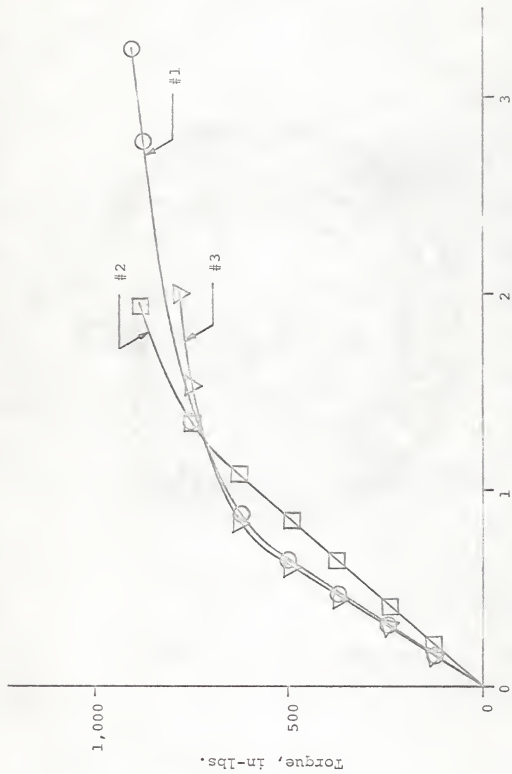
Unit Angle of Twist, 1×10^{-2} radians

FIGURE 22. TORQUE-TWIST CURVES FOR BEAMS 1.4-0.4



Unit Angle of Twist, 1×10^{-2} radians

FIGURE 23. TORQUE-TWIST CURVES FOR BEAMS 1.4-0.5



Unit Angle of Twist, 1×10^{-2} radians

FIGURE 24. TORQUE-TWIST CURVES FOR BEAMS 1.4-0.6

SMALL SCALE MODEL ANALYSIS OF
REINFORCED CONCRETE BEAMS IN
FLEXURE AND IN TORSION

by

GARY E. MASON

B. S., Kansas State University, 1964

AN ABSTRACT OF A MASTER'S THESIS

submitted in partial fulfillment of the

requirements for the degree

MASTER OF SCIENCE

Department of Civil Engineering

KANSAS STATE UNIVERSITY

1967

ABSTRACT

The primary purpose of this investigation was to determine if model reinforced concrete beams could be used experimentally to predict the behavior of prototype beams in flexure and in torsion. The physical properties of the "Ultracal 30" mix used as a substitute for concrete and of the various wire used as reinforcement were established.

The results of the model tests were compared with Whitney's theory for the ultimate strength of reinforced concrete beams in flexure and with Lessig's theory for the ultimate strength of reinforced concrete beams in torsion. The flexure specimens contained only threaded rod used as longitudinal reinforcement. The torsion specimens contained the threaded rod for longitudinal reinforcement and also smooth wire for transverse reinforcement.

The flexural experiments were designed to allow a statistical analysis of the data for certain cross-section-span combinations. The torsion experiment was designed for a range of cross-section-m combinations where m is the ratio of transverse force to longitudinal force in the reinforcing steel.

The results from the flexure tests agreed very well with Whitney's theory. The results from the torsion tests did not agree with the ultimate strength predicted by Lessig's theory. It is believed that the torsion test apparatus applied a degree of fixity to the ends of the beams due to misalignment.